



Published in final edited form as:

Muscle Nerve. 2010 November ; 42(5): 722–730. doi:10.1002/mus.21743.

ACTIVIN IIB RECEPTOR BLOCKADE ATTENUATES DYSTROPHIC PATHOLOGY IN A MOUSE MODEL OF DUCHENNE MUSCULAR DYSTROPHY

Kevin J. Morine, MD¹, Lawrence T. Bish, BA¹, Joshua T. Selsby, PhD², Jeffery A. Gazzara¹, Klara Pendrak, PhD¹, Meg M. Sleeper, VMD³, Elisabeth R. Barton, PhD⁴, Se-Jin Lee, MD, PhD⁵, and H. Lee Sweeney, PhD¹

¹Department of Physiology, University of Pennsylvania School of Medicine, 3615 Civic Center Boulevard, 1115 Abramson Center, Philadelphia, Pennsylvania 19104, USA

²Department of Animal Science, Iowa State University, Ames, Iowa, USA

³Section of Cardiology, University of Pennsylvania School of Veterinary Medicine, Philadelphia, Pennsylvania, USA

⁴Department of Anatomy and Cell Biology, University of Pennsylvania School of Dental Medicine, Philadelphia, Pennsylvania, USA

⁵Department of Molecular Biology and Genetics, Johns Hopkins University, Baltimore, Maryland, USA

Abstract

Modulation of transforming growth factor- β (TGF- β) signaling to promote muscle growth holds tremendous promise for the muscular dystrophies and other disorders involving the loss of functional muscle mass. Previous studies have focused on the TGF- β family member myostatin and demonstrated that inhibition of myostatin leads to muscle growth in normal and dystrophic mice. We describe a unique method of systemic inhibition of activin IIB receptor signaling via adeno-associated virus (AAV)-mediated gene transfer of a soluble form of the extracellular domain of the activin IIB receptor to the liver. Treatment of *mdx* mice with activin IIB receptor blockade led to increased skeletal muscle mass, increased force production in the extensor digitorum longus (EDL), and reduced serum creatine kinase. No effect on heart mass or function was observed. Our results indicate that activin IIB receptor blockade represents a novel and effective therapeutic strategy for the muscular dystrophies.

Keywords

activin IIB receptor; adenoassociated virus; gene therapy; muscular dystrophy; transforming growth factor- β

Duchenne muscular dystrophy is characterized by progressive deterioration of skeletal muscle due to the absence of dystrophin. Although no definitive treatment is yet available,

considerable attention has been devoted to treatments that increase functional muscle mass by enhancing growth or preventing breakdown. As dystrophic muscle is inherently susceptible to contraction-induced damage, it is conceivable that increasing muscle mass would reduce relative load on the muscle and decrease damage during routine use. Two approaches that have been previously explored in non-dystrophic mice to induce muscle hypertrophy include increased expression of insulinlike growth factor-1 (IGF-1), a positive growth factor, and inhibition of myostatin, a negative growth factor.^{1,2} Although we and others have successfully exploited the myostatin signaling pathways to ameliorate murine dystrophic pathology it is unclear if these results translate to humans.³⁻⁵ Indeed, a recent clinical trial that utilized a recombinant myostatin antibody failed to demonstrate clinical improvement in adult muscular dystrophies.⁶ Novel strategies that promote muscle growth may be beneficial for treatment of the muscular dystrophies as well as disuse atrophy, sarcopenia, cachexia, and other muscle wasting disorders.

The transforming growth factor- β (TGF- β) superfamily of growth factors are circulating polypeptides implicated in the control of diverse biological functions. Members of the TGF- β family act as ligands for heteromers of membrane-associated type I and II receptors, which possess cytoplasmic serine/threonine kinase domains.⁷ These domains phosphorylate and activate intracellular mediators such as the Smads, which translocate to the nucleus upon activation and directly modulate transcription.⁸ More than 30 TGF- β ligands have been identified. Only five type II receptors have been characterized, which indicates each type II receptor mediates signaling for multiple ligands.⁹ The type II receptors for activin include activin IIAr and IIBr.^{10,11} These receptors have generated considerable interest for their widespread involvement in embryonic development and postnatal regulation of varied processes, including osteogenesis, vasculogenesis, and skeletal muscle growth.¹² In the developing mouse, the activin IIB receptor is expressed in the embryonic ectoderm during gastrulation and has been detected in a variety of embryonic organs, including the brain, stomach, and metanephros.^{11,13} Absence of the activin IIB receptor in transgenic mice leads to patterning defects and is perinatally lethal secondary to cardiovascular abnormalities in the majority of receptor-deficient mice.¹⁴ The *in vivo* ligands for activin IIBr include activin, inhibin, members of the bone morphogenetic protein (BMP) family, myostatin, and growth and differentiation factor 11 (GDF11).^{15,16}

The control mechanism of muscle growth by activin receptor signaling pathways is not completely defined. Through various experimental modalities and multiple animal models, myostatin genetic deletion or postnatal inhibition results in muscle growth.^{2,3,17} Interestingly, myostatin knockout mice gained an additional 15–26% of muscle mass when injected with a soluble form of the activin IIB receptor.¹⁸ Further, muscle mass is nearly quadrupled in a transgenic cross between the myostatin knockout and a skeletal muscle specific overexpression of follistatin.¹⁹ Thus, there is at least one other circulating factor that signals through the activin IIB receptor and negatively regulates muscle mass. Affinity purification studies of mouse and human serum utilizing the activin IIB receptor as bait revealed that activin A/B, GDF8/myostatin, and GDF11 circulate in normal serum and are capable of blocking *in vitro* myoblast differentiation.¹⁶ Of these factors, only myostatin has conclusively been shown to regulate muscle mass *in vivo*. GDF11 is unlikely to be a candidate negative regulator, as the skeletal muscle specific loss of GDF11 did not affect

muscle size.²⁰ A recent study showed a 15% decrease in muscle mass following activin A overexpression in rat muscle, implicating activin A as a potential regulator of muscle mass.²¹ Other additional factors, either activin or undiscovered ligands, may be responsible for regulation of muscle size and, along with myostatin, may contribute to activin IIB receptor blockade-mediated muscle growth.

In transgenic mice that express a truncated activin IIB receptor under control of a muscle-specific promoter, up to a 125% increase in skeletal muscle mass was observed at 7 months of age.²² These mice were crossed with *mdx* mice, and the resulting mice were found to have qualitatively larger muscles and improved myoblast transplantation efficiency.²³ It is not clear from this study that activin IIB receptor blockade improves dystrophic pathology, as markers of disease progression, such as force production, fibrosis, and serum creatine kinase levels, were not reported. Injection of a soluble form of the activin IIB extracellular domain led to a 60% increase in skeletal muscle mass in normal mice and in a mouse model of amyotrophic lateral sclerosis by increasing skeletal muscle fiber size.^{18,24} Similarly, administration of recombinant activin IIB receptor to caveolin-3-deficient mice countered some muscle atrophy.²⁵ Those studies showed that activin IIB receptor blockade increases skeletal muscle mass; however, a comprehensive functional evaluation of the effect of this approach on muscular dystrophy has not yet been reported.

To determine whether activin IIB receptor blockade is potentially therapeutic for muscular dystrophy, the effect of liver-mediated expression of a novel activin receptor inhibitor on muscle mass and function in the *mdx* mouse model of Duchenne muscular dystrophy was assessed. Young *mdx* mice were injected with adeno-associated virus (AAV) containing a liver-specific promoter (LSP) and a transgene consisting of a soluble form of the activin IIB receptor fused to the fixed-chain region of IgG2a. At 5 months of age, a histological and functional assessment of the soleus, extensor digitorum longus (EDL), and diaphragm was made. Increased muscle mass was observed in all limb muscles with the exception of the soleus. Increased absolute but not specific force production was found in the EDL, whereas no changes were observed in the soleus or diaphragm. Analysis of muscle morphology revealed that muscle growth in the EDL was due to hypertrophy without hyperplasia. Echocardiography demonstrated no effect of the activin inhibitor on cardiac function. Although long-term studies are necessary, these results indicate activin receptor blockade is a safe and effective strategy for improving muscle size and function in muscular dystrophy.

METHODS

Vector Production

The activin IIB receptor-IgG2a extracellular domain fusion construct was subcloned into an AAV transfer vector with the α_1 -antitrypsin promoter with ApoE enhancer.¹⁸ The soluble activin receptor construct consists of the mouse myostatin signal sequence, the extracellular domain of the activin IIB receptor, and the fixed-chain region of IgG2a. Standard inverted terminal repeats (ITRs) flank the construct to permit packaging into AAV pseudotype 2/8. This promoter is liver-specific (abbreviated LSP) and was provided by Dr. Katherine High. AAV pseudotype 2/8 was produced by the University of Pennsylvania Vector Core as previously described.²⁶

Viral Injection of Mice

All animal experiments were approved by the University of Pennsylvania Animal Care and Use Committee. Six-week-old male *mdx* mice ($n = 5$ control, $n = 5$ treated) were injected with 1×10^{12} genome copies of AAV 2/8 LSP.sActIIBr or saline via intraperitoneal injection. Following sedation with a ketamine–xylazine mixture, mice were injected intraperitoneally in the left lower quadrant of the abdomen with 1×10^{12} genome copies of virus diluted in 300 μ l of saline or 300 μ l of saline for controls. Mice were killed at 5 months of age and analyzed as described in what follows.

Muscle Morphology

For morphological analysis, muscles were embedded in optimal cutting temperature compound (Sakura Finetek, Torrance, California) and frozen in liquid nitrogen–cooled isopentane. Ten-micron-thick sections were cut, and the resulting slides were stored at -20°C . Immunohistochemistry was employed to determine the fiber sizes, fiber number, and myosin heavy chain (MHC) composition of the examined muscles, as described previously.³ The MHC antibodies used to determine the MHC composition of selected muscles were type I (BA-F8) at 1:50, type IIA (SC-71) at 1:10, and type IIB (BF-F3) at 1:3. Sections were blocked in 5% bovine serum albumin/ phosphate-buffered saline (BSA/PBS) and incubated overnight in 5% BSA/PBS containing rabbit anti-laminin monoclonal antibody diluted 1:100 (Neomarkers, Fremont, California) and an MHC primary antibody at the dilutions described earlier. Following washes in PBS, sections were incubated in appropriate secondary antibodies (Invitrogen, Carlsbad, California) for 1 hour in the dark at room temperature. Slides were washed and mounted with VectaShield with 4'-6-diamidino-2-phenylindole (DAPI). All images were captured and processed on a fluorescence microscope (Leitz DMRBE; Leica, Bannockburn, Illinois) equipped with a digital camera system (MicroMAX; Princeton Instruments, Trenton, New Jersey). Imaging software (OpenLab; Improvision, Waltham, Massachusetts) was used for quantification of fiber size. Centrally nucleated fibers were counted as fibers where the nucleus was closer to the center of the fiber than the periphery. The number of centrally nucleated fibers is presented as a percentage of the total number of fibers present in the muscle section.

Immunoblotting

For western blotting, muscles were dissected, weighed, and snap-frozen in liquid nitrogen. Muscles were crushed in a mortar and pestle on dry ice. Samples were then homogenized in lysis buffer [5 mM ethylene-diamine tetraacetic acid (pH 8), 50 mM Tris-Cl (pH 8), 150 mM NaCl, 0.1% sodium dodecylsulfate (SDS), 1% Triton X-100, 0.5% deoxycholate, 50 mM dithiothreitol (DTT), and Complete Protease Inhibitor Cocktail (Roche, Indianapolis, Indiana)]. Following incubation on ice for 10 min the protein homogenates were centrifuged at 12,000 rpm for 10 min. The supernatant was used for subsequent western blotting. Protein concentration was determined by protein assay (Bio-Rad, Hercules, California). Fifty micrograms of protein or 1.5 μ l of serum was mixed with 2 \times SDS loading buffer [130 mM Tris (pH 8), 20% glycerol, 4.6% SDS, 2% DTT, 0.02% bromophenol blue], denatured at 95°C for 10 min, and loaded onto 4–20% precast gels (PAGEr Gold; Lonza, Rockland, Maine). Proteins were transferred via the iBlot Dry Blotting System onto nitrocellulose

membranes (Invitrogen, Carlsbad, California). The membrane was then blocked with 5% nonfat dry milk in Tris-buffered saline containing 0.05% Tween 20. Immunoblotting was performed to detect activin IIB receptor (1:1000; Sigma, St. Louis, Missouri) and actin (1:2000; Sigma). Appropriate horseradish peroxidase–conjugated secondary antibodies were used at twice the dilution of primary antibody (GE Healthcare, UK). Protein detection was performed by exposure to chemiluminescence (Super Signal West Pico Chemiluminescent Substrate Kit; Pierce, Rockford, Illinois), and signal quantification was processed using densitometry software (Alpha Innotech, San Leandro, California).

Serum Creatine Kinase Activity

Serum creatine kinase (CK) levels were assessed with the indirect CK colorimetric assay kit according to the manufacturer's protocol (Sigma).

Muscle Functional Analysis

The contractile properties of the soleus, extensor digitorum longus (EDL), and diaphragm were measured. Mice were anesthetized with ketamine/xylazine (80 and 10 mg/kg body weight, respectively) and exsanguinated. Blood samples were allowed to clot, centrifuged at $2000 \times g$ for 20 min, and then stored at -80°C for measurement of serum CK and circulating activin receptor. The EDL, soleus, diaphragm, quadriceps, and gastrocnemius muscles were removed and placed in a bath of Ringer solution gas equilibrated with 95% O_2 /5% CO_2 . The EDL, soleus, and diaphragm muscles were subjected to isolated mechanical measurements using a previously described apparatus (Aurora Scientific, Ontario, Canada).²⁷ After determining optimum length (L_o) by supramaximal twitch stimulation, maximum isometric tetanus was measured. Upon completion of these measurements, muscles were weighed and rapidly frozen in melting isopentane for morphological analysis.

In Vivo Transthoracic Echocardiography

M-mode echocardiography was performed on *mdx* animals under ketamine/xylazine anesthesia using a 15-MHZ phased-array probe connected to an echocardiographic machine (Sonos 7500; Philips Medical Imaging, Andover, Massachusetts). In brief, an M-mode cursor was positioned in the parasternal short-axis view perpendicular to the interventricular septum and posterior wall of the left ventricle (LV) at the level of the papillary muscles, and M-mode images were obtained for measurement of LV end-diastolic and end-systolic dimension (LVDD and LVDs). The percentage of fractional shortening (%FS) was calculated from the equation: $\%FS = [(LVDD - LVDs) / LVDD] \times 100$. The end-diastolic and end-systolic volumes, ejection fraction, cardiac output, and stroke volume were calculated using the Teicholtz formulas.²⁸ The same sonographer (M.S.), who was blinded to the treatment groups of the mice, performed all studies and the resulting calculations.

Statistical Analysis

The two-tailed unpaired Student's *t*-test was used to compare means between experimental groups. Numerical data are reported as mean \pm standard deviation. $P < 0.05$ was considered significant.

RESULTS

The tissue distribution of the activin IIB receptor in the adult mouse was assessed by immunoblotting to determine what organ systems may be sensitive to activin IIB receptor blockade (Fig. 1a). The activin IIB receptor was expressed in a diversity of tissues as observed in the zebrafish and was found at the highest levels in the brain, heart, and skeletal muscle.²⁹ The fast-twitch EDL notably contained more receptor than the slow-twitch soleus. The difference in receptor density may underlie the variance in phenotype of these muscles in the myostatin knockout mouse and their responsiveness to myostatin inhibition in adult animals.³⁰ A viral construct was then designed to constitutively express a soluble form of the activin IIB receptor specifically from the liver (Fig. 1b). The liver-specific α_1 -antitrypsin promoter with apoE enhancer (LSP), previously used in our laboratory to express the myostatin propeptide from the liver, was paired with a soluble activin inhibitor.³¹ The inhibitor consists of the extracellular domain of the activin IIB receptor fused to the signal sequence from the mouse myostatin gene (sActIIBr). The fixed-chain region of IgG2a was appended to the inhibitor to confer additional stability to the recombinant protein.³²

Six-week-old *mdx* mice ($n = 5$ controls, $n = 5$ treated) were injected with 1E12 genome copies of AAV 2/8 LSP.sActIIBr. Immunoblotting of serum samples 1 month after injection for activin IIBr demonstrated sActIIBr in the circulation (Fig. 1c). Quantitative immunoblotting using purified sActIIBr as a standard demonstrated that the amount of sActIIBr in the circulation of treated mice was 1.5 ± 1.6 ng/ μ l. In treated *mdx* mice, we observed increased body weight beginning at 1 month post-injection and continuing until the termination of the study at 5 months of age (Fig. 1d). Serum CK, a marker of membrane permeability and muscle damage, was reduced in the *mdx*/sActIIBr group (Fig. 1e). Reduced serum CK was also observed in short-term studies of myostatin inhibition in *mdx* mice, although the mechanism of this benefit is unclear.^{4,33,34}

Activin receptor blockade resulted in increased weight of all skeletal muscles examined, with the exception of the soleus (Fig. 2). The gastrocnemius, tibialis anterior, and quadriceps had 39%, 46%, and 39% greater muscle mass than control, respectively (Fig. 2a). The EDL, a fast skeletal muscle, was 31% heavier, whereas the soleus, a slow skeletal muscle, was not significantly heavier (Fig. 2b). Muscle weights were normalized to body weight, and the ratio was increased in the gastrocnemius, tibialis anterior, and quadriceps (Fig. 2c). The muscle weight/body weight ratio was unchanged in the EDL and soleus (Fig. 2d). Heart weight and heart weight/body weight ratio were not affected by expression of sActIIBr (Fig. 2a, c).

As the dystrophic process proceeds at different trajectories in different muscle groups, a functional and morphological analysis of representative muscles was undertaken. The EDL contains a large number of fast glycolytic fibers that express MHC type IIB and was selected as a fast muscle type. Similarly, the soleus contains a large proportion of slow oxidative fibers that express MHC type I and was chosen as a slow muscle type. The diaphragm is a severely affected skeletal muscle in the *mdx* mouse and recapitulates the course of the human disease.³⁵ Also, the diaphragm contains a mixed population of fiber types consisting of mostly MHC type IIA/IIX fibers and is uniquely adapted to persistent use.³⁶

The functional properties of the EDL, soleus, and diaphragm were measured at the conclusion of the study (Fig. 3). In the *mdx/sActIIBr* group, the EDL exhibited 31% larger cross-sectional area (CSA) and 28% greater tetanic force production (Fig. 3b, c). Importantly, specific force, or tetanic force normalized to CSA, was not compromised by sActIIBr overexpression (16.4 ± 3.6 in control *mdx* vs. 16.2 ± 2.4 N/cm² in *mdx/sActIIBr*). The soleus demonstrated similar CSA (1.53 ± 0.17 vs. 1.65 ± 0.18 mm²), tetanic force production (223 ± 54 vs. 266 ± 52 mN), and specific force (14.6 ± 3.4 vs. 16.2 ± 3.1 N/cm²). No difference in specific force was observed in the diaphragm (5.6 ± 0.8 vs. 5.5 ± 0.4 N/cm²).

To determine the mechanism of muscle growth mediated by activin receptor blockade, morphological analysis of representative muscle groups was undertaken. The EDL exhibited increased mean fiber size (Fig. 3a) without change in fiber number (828 ± 209 vs. 870 ± 90 fibers). These results indicate that muscle growth was due to hypertrophy without hyperplasia in the EDL. Sagittal fiber number (11.8 ± 2.5 vs. 12.3 ± 2.3 fibers) and the mean fiber size of type I, type IIA, type IIB, and total fibers in the diaphragm were not altered by overexpression of sActIIBr (Fig. 3d). The proportion of centrally nucleated fibers, an indicator of previously regenerated fibers, were assessed and found to be unchanged in the *mdx/sActIIBr* EDL ($57.6 \pm 6\%$ vs. $54.3 \pm 8\%$ of total fibers) and diaphragm (13.3 ± 6.5 vs. 13.3 ± 2.5 percent of total fibers). Thus, activin blockade did not alter any measured parameter in the diaphragm and increased muscle fiber size in the EDL. Fiber size, fiber number, MHC composition, and the proportion of centrally nucleated fibers were unaltered in the *mdx/sActIIBr* soleus (data not shown).

As the activin IIB receptor is expressed in the heart at levels comparable to skeletal muscle, we investigated whether there was any functional effect of activin blockade on the heart at the study endpoint by echocardiography. No differences were observed in heart rate (419 ± 53 in control *mdx* vs. 374 ± 60 in *mdx/sActIIBr*), LV inner dimension at diastole (0.33 ± 0.02 vs. 0.36 ± 0.05), LV inner dimension at systole (0.2 ± 0.04 vs. 0.24 ± 0.06), end-diastolic volume (0.09 ± 0.02 vs. 0.13 ± 0.05), or end-systolic volume (0.03 ± 0.01 vs. 0.04 ± 0.03). Also, fractional shortening ($38 \pm 7.5\%$ vs. $35 \pm 7.0\%$) and ejection fraction (74 ± 8.1 vs. 73 ± 10.4) were unchanged. These data indicate that overexpression of circulating sActIIBr did not affect cardiac function in young *mdx* mice.

DISCUSSION

This study is the first demonstration of the effect of activin receptor blockade in a model of Duchenne muscular dystrophy. The soluble activin receptor approach has been exploited to increase muscle growth in normal mice and models of primary neurological disorders to varying effect.^{18,24,37} Herein we have shown that liver-mediated expression of a soluble activin IIB inhibitor in *mdx* mice leads to increased muscle size and strength as well as reduced serum CK levels. Numerous studies have shown beneficial effects of myostatin inhibition on mild muscular dystrophy as typified by the *mdx* model.^{4,17,33} However, early enthusiasm for this approach has been tempered by equivocal results in more severe mouse models and humans.^{6,33,38} In comparison to myostatin-specific inhibition, the activin IIB receptor binds to and is capable of inhibiting additional ligands such as activin, inhibin, and

GDF11.¹⁶ GDF11 and activin A/B have been shown to influence myotube differentiation in vitro, yet definitive evidence of their role in the regulation of muscle formation or size in vivo is lacking.^{16,20} Modulation of these divergent signaling pathways may additively increase muscle mass and delay the pathological progression of muscular dystrophy. It should be emphasized that interventions that increase muscle size without stabilization of the sarcolemma do not appear to alter the inherent susceptibility of dystrophic muscle to contraction-induced damage.³ Rather, the number of motor units required to produce a given amount of force is reduced. As contraction-induced damage is thought to be the predominant mechanism of muscle loss in muscular dystrophy, reducing the number of motor units recruited to produce force may slow the loss of functional muscle mass.³⁹

The increased skeletal muscle mass observed in our study was due to hypertrophy without hyperplasia and is comparable to prior studies of myostatin inhibition studies in *mdx* mice.^{17,33} The EDL, a representative fast muscle type, responded more robustly to activin receptor blockade than the soleus, a representative slow muscle type, as demonstrated by an increase in muscle weight and mean fiber size. The increased weight of the EDL occurred via an increase in size of existing fibers (hypertrophy) without a change in the number of muscle fibers (hyperplasia). Muscle growth due to hypertrophy and not hyperplasia is consistent with prior studies of postnatal myostatin inhibition.^{40,41} The EDL displayed increased absolute force production with no change in force production normalized to CSA (specific force). Thus, activin blockade increases muscle size in fast-twitch muscle without the compromised contractile function seen in the myostatin knockout EDL.⁴² In contrast, the soleus and diaphragm did not show any change in fiber size or muscle strength. Fast muscle fibers and muscle types appear to preferentially respond to the absence or postnatal inhibition of myostatin, as observed in the myostatin knockout mouse and studies of myostatin inhibition in the *mdx* mouse.^{30,31,43} The etiology of the reduced response in the soleus and slow muscle fibers is unknown; however, it may be related to the fiber type-dependent differential expression of the activin IIB receptor, as reported here and elsewhere.³⁰ An equally plausible explanation for the observed non-responsiveness to activin receptor blockade in the diaphragm is that aerobic adaptation to persistent use limits the capacity of the fast fibers to hypertrophy. The fast fibers in the diaphragm are uniquely adapted for constant use and are dependent on oxygen diffusion and consumption for adenosine triphosphate production.³⁶ In contrast, the EDL contains fast fibers dependent on glycolytic metabolism for energy production. Hence, it is possible that the equivalent fast fibers in the diaphragm will not respond as robustly to activin receptor blockade due to a size limitation imposed by aerobic dependence.

Although activin IIB receptor blockade leads to massive skeletal muscle hypertrophy and ameliorates some aspects of dystrophic pathology, the potential effects in other organ systems should be addressed in future studies. The activin IIB receptor approach or expression of other circulating binding proteins, such as follistatin, follistatin-related gene (FLRG), and growth and differentiation factor-1 (GASP-1), do generate rapid and impressive gains in muscle mass. However, long-term use may be precluded by impaired signaling of other TGF- β family members.^{22,44–46} The activin IIB receptor is expressed in the brain, heart, liver, and gonads, as well as in skeletal muscle of the zebrafish, and has a

similarly diverse expression profile in the adult mouse (Fig. 1).²⁹ The broad tissue distribution of the activin IIB receptor and its diverse ligands suggest complete interference with signaling through the receptor may result in maladaptive abnormalities in other organ systems such as the liver, pancreas, and gonads. For example, adenoviral expression of a truncated activin IIB receptor in the liver resulted in transiently increased liver weight and decreased serum cholesterol and albumin.⁴⁷ Analysis of activin IIB receptor– deficient mice crossed to Smad2-deficient mice revealed smaller pancreatic islet size and reduced insulin content.⁴⁸ Studies of the TGF- β antagonist follistatinlike-3 transgenics revealed potentially adverse effects on metabolic homeostasis and reproductive function.^{49,50} Another consideration is the effect of reduced activin receptor signaling on the heart. The influence of activin IIB receptor ligands, such as myostatin, on cardiac size and function is disputed.^{51,52} Our findings indicate activin receptor blockade has no acute effect on cardiac function. To ensure the safety of this approach on normal and dystrophic cardiac physiology, long-term studies are required.

Activin receptor blockade is a potential therapeutic modality for a wide range of muscle disorders that should be further investigated in preclinical studies. The response of murine dystrophic models to myostatin inhibition has been variable depending on the nature of the primary defect and severity of disease progression.^{38,53,54} Activin receptor blockade, by inhibiting additional activin receptor ligands, may afford greater resistance to dystrophic damage than myostatin inhibition alone. For Duchenne muscular dystrophy, canine models that accurately recapitulate the course of human disease are available to test the efficacy of activin blockade.^{55,56} As therapeutic liver transduction by AAV has been shown in a canine model of hemophilia B, it is feasible that our approach could be translated to a dystrophic dog model by creating a species-specific transgene.⁵⁷ Aberrant signaling through the activin receptors has been implicated in many other disorders such as cachexia, diabetes, disuse atrophy, and sarcopenia.⁵⁸ Although the effect of myostatin inhibition has been described in some of these disease states, further benefit may accrue with more complete activin receptor inhibition as is likely achieved with our method. Additional studies are underway to directly compare the effect of postnatal myostatin inhibition and activin receptor blockade in normal and dystrophic mice.

Acknowledgments

This work was supported by a grant from a Wellstone Muscular Dystrophy Cooperative Center (U54-AR052646) to H.L.S.

Abbreviations

| | |
|------------|----------------------------|
| AAV | adeno-associated virus |
| BMP | bone morphogenetic protein |
| BSA | bovine serum albumin |
| CK | creatine kinase |
| CSA | cross-sectional area |

| | |
|-------------------------------|--------------------------------------|
| DAPI | 4'-6-diamidino-2-phenylindole |
| DTT | dithiothreitol |
| EDL | extensor digitorum longus |
| FLRG | follastin-related gene |
| GDF11 | growth and differentiation factor 11 |
| IGF-1 | insulinlike growth factor-1 |
| ITR | inverted terminal repeat |
| LSP | liver-specific promoter |
| LV | left ventricle |
| LVd | left ventricular end-diastolic |
| LVDs | left ventricular end-diastolic |
| MHC | myosin heavy chain |
| PBS | phosphate-buffered saline |
| sActIIBr | soluble activin IIB receptor |
| SDS | sodium dodecylsulfate |
| TGF-β | transforming growth factor- β |

REFERENCES

1. Musaro A, McCullagh K, Paul A, Houghton L, Dobrowolny G, Molinaro M, et al. Localized Igf-1 transgene expression sustains hypertrophy and regeneration in senescent skeletal muscle. *Nat Genet.* 2001; 27:195–200. [PubMed: 11175789]
2. Whittemore LA, Song K, Li X, Aghajanian J, Davies M, Girgenrath S, et al. Inhibition of myostatin in adult mice increases skeletal muscle mass and strength. *Biochem Biophys Res Commun.* 2003; 300:965–971. [PubMed: 12559968]
3. Barton ER, Morris L, Musaro A, Rosenthal N, Sweeney HL. Muscle-specific expression of insulin-like growth factor I counters muscle decline in mdx mice. *J Cell Biol.* 2002; 157:137–148. [PubMed: 11927606]
4. Bogdanovich S, Krag TO, Barton ER, Morris LD, Whittemore LA, Ahima RS, et al. Functional improvement of dystrophic muscle by myostatin blockade. *Nature.* 2002; 420:418–421. [PubMed: 12459784]
5. Schertzer JD, Ryall JG, Lynch GS. Systemic administration of IGF-I enhances oxidative status and reduces contraction-induced injury in skeletal muscles of mdx dystrophic mice. *Am J Physiol Endocrinol Metab.* 2006; 291:E499–E505. [PubMed: 16621899]
6. Wagner KR, Fleckenstein JL, Amato AA, Barohn RJ, Bushby K, Escolar DM, et al. A phase I/II trial of MYO-029 in adult subjects with muscular dystrophy. *Ann Neurol.* 2008; 63:561–571. [PubMed: 18335515]
7. de Caestecker M. The transforming growth factor-beta superfamily of receptors. *Cytokine Growth Factor Rev.* 2004; 15:1–11. [PubMed: 14746809]
8. Massague J. How cells read TGF-beta signals. *Nat Rev Mol Cell Biol.* 2000; 1:169–178. [PubMed: 11252892]
9. Schmierer B, Hill CS. TGFbeta-SMAD signal transduction: molecular specificity and functional flexibility. *Nat Rev Mol Cell Biol.* 2007; 8:970–982. [PubMed: 18000526]

10. Mathews LS, Vale WW. Expression cloning of an activin receptor, a predicted transmembrane serine kinase. *Cell*. 1991; 65:973–982. [PubMed: 1646080]
11. Manova K, De Leon V, Angeles M, Kalantry S, Giarre M, Attisano L, et al. mRNAs for activin receptors II and IIB are expressed in mouse oocytes and in the epiblast of pregastrula and gastrula stage mouse embryos. *Mech Dev*. 1995; 49:3–11. [PubMed: 7748787]
12. Tsuchida K, Nakatani M, Uezumi A, Murakami T, Cui X. Signal transduction pathway through activin receptors as a therapeutic target of musculoskeletal diseases and cancer. *Endocrine J*. 2008; 55:11–21. [PubMed: 17878607]
13. Feijen A, Goumans MJ, van den Eijnden-van Raaij AJ. Expression of activin subunits, activin receptors and follistatin in postimplantation mouse embryos suggests specific developmental functions for different activins. *Development*. 1994; 120:3621–3637. [PubMed: 7821227]
14. Oh SP, Li E. The signaling pathway mediated by the type IIB activin receptor controls axial patterning and lateral asymmetry in the mouse. *Genes Dev*. 1997; 11:1812–1826. [PubMed: 9242489]
15. Attisano L, Wrana JL, Cheifetz S, Massague J. Novel activin receptors: distinct genes and alternative mRNA splicing generate a repertoire of serine/threonine kinase receptors. *Cell*. 1992; 68:97–108. [PubMed: 1310075]
16. Souza TA, Chen X, Guo Y, Sava P, Zhang J, Hill JJ, et al. Proteomic identification and functional validation of activins and bone morphogenetic protein 11 as candidate novel muscle mass regulators. *Mol Endocrinol*. 2008; 22:2689–2702. [PubMed: 18927237]
17. Wagner KR, McPherron AC, Winik N, Lee SJ. Loss of myostatin attenuates severity of muscular dystrophy in mdx mice. *Ann Neurol*. 2002; 52:832–836. [PubMed: 12447939]
18. Lee SJ, Reed LA, Davies MV, Girgenrath S, Goad ME, Tomkinson KN, et al. Regulation of muscle growth by multiple ligands signaling through activin type II receptors. *Proc Natl Acad Sci USA*. 2005; 102:18117–18122. [PubMed: 16330774]
19. Lee SJ. Quadrupling muscle mass in mice by targeting TGF-beta signaling pathways. *PLoS One*. 2007; 2:e789. [PubMed: 17726519]
20. McPherron AC, Huynh TV, Lee SJ. Redundancy of myostatin and growth/differentiation factor 11 function. *BMC Dev Biol*. 2009; 9:24. [PubMed: 19298661]
21. Gilson H, Schakman O, Kalista S, Lause P, Tsuchida K, Thissen JP. Follistatin induces muscle hypertrophy through satellite cell proliferation and inhibition of both myostatin and activin. *Am J Physiol Endocrinol Metab*. 2009; 297:E157–E164. [PubMed: 19435857]
22. Lee SJ, McPherron AC. Regulation of myostatin activity and muscle growth. *Proc Natl Acad Sci USA*. 2001; 98:9306–9311. [PubMed: 11459935]
23. Benabdallah BF, Bouchentouf M, Tremblay JP. Improved success of myoblast transplantation in mdx mice by blocking the myostatin signal. *Transplantation*. 2005; 79:1696–1702. [PubMed: 15973171]
24. Morrison BM, Lachey JL, Warsing LC, Ting BL, Pullen AE, Underwood KW, et al. A soluble activin type IIB receptor improves function in a mouse model of amyotrophic lateral sclerosis. *Exp Neurol*. 2009; 217:258–268. [PubMed: 19285073]
25. Ohsawa Y, Hagiwara H, Nakatani M, Yasue A, Moriyama K, Murakami T, et al. Muscular atrophy of caveolin-3-deficient mice is rescued by myostatin inhibition. *J Clin Invest*. 2006; 116:2924–2934. [PubMed: 17039257]
26. Gao GP, Alvira MR, Wang L, Calcedo R, Johnston J, Wilson JM. Novel adeno-associated viruses from rhesus monkeys as vectors for human gene therapy. *Proc Natl Acad Sci USA*. 2002; 99:11854–11859. [PubMed: 12192090]
27. Barton ER. Impact of sarcoglycan complex on mechanical signal transduction in murine skeletal muscle. *Am J Physiol Cell Physiol*. 2006; 290:C411–C419. [PubMed: 16162659]
28. Silcocks PB, Munro JF, Steeds RP, Channer KS. Prognostic implications of qualitative assessment of left ventricular function compared to simple routine quantitative echocardiography. *Heart*. 1997; 78:237–242. [PubMed: 9391284]
29. Garg RR, Bally-Cuif L, Lee SE, Gong Z, Ni X, Hew CL, et al. Cloning of zebrafish activin type IIB receptor (ActRIIB) cDNA and mRNA expression of ActRIIB in embryos and adult tissues. *Mol Cell Endocrinol*. 1999; 153:169–181. [PubMed: 10459865]

30. Mendias CL, Marcin JE, Calderon DR, Faulkner JA. Contractile properties of EDL and soleus muscles of myostatin-deficient mice. *J Appl Physiol*. 2006; 101:898–905. [PubMed: 16709649]
31. Morine KJ, Bish LT, Pendrak K, Sleeper MM, Barton ER, Sweeney HL. Systemic myostatin inhibition via liver-targeted gene transfer in normal and dystrophic mice. *PLoS One*. 2010; 5:e9176. [PubMed: 20161803]
32. Wolfman NM, McPherron AC, Pappano WN, Davies MV, Song K, Tomkinson KN, et al. Activation of latent myostatin by the BMP-1/tolloid family of metalloproteinases. *Proc Natl Acad Sci USA*. 2003; 100:15842–15846. [PubMed: 14671324]
33. Bogdanovich S, Perkins KJ, Krag TO, Whittemore LA, Khurana TS. Myostatin propeptide-mediated amelioration of dystrophic pathophysiology. *FASEB J*. 2005; 19:543–549. [PubMed: 15791004]
34. Qiao C, Li J, Jiang J, Zhu X, Wang B, Xiao X. Myostatin propeptide gene delivery by adeno-associated virus serotype 8 vectors enhances muscle growth and ameliorates dystrophic phenotypes in mdx mice. *Hum Gene Ther*. 2008; 19:241–254. [PubMed: 18288893]
35. Stedman HH, Sweeney HL, Shrager JB, Maguire HC, Panettieri RA, Petrof B, et al. The mdx mouse diaphragm reproduces the degenerative changes of Duchenne muscular dystrophy. *Nature*. 1991; 352:536–539. [PubMed: 1865908]
36. Polla B, D'Antona G, Bottinelli R, Reggiani C. Respiratory muscle fibres: specialisation and plasticity. *Thorax*. 2004; 59:808–817. [PubMed: 15333861]
37. Sumner CJ, Wee CD, Warsing LC, Choe DW, Ng AS, Lutz C, et al. Inhibition of myostatin does not ameliorate disease features of severe SMA mice. *Hum Mol Genet*. 2009; 18:3145–3152. [PubMed: 19477958]
38. Bogdanovich S, McNally EM, Khurana TS. Myostatin blockade improves function but not histopathology in a murine model of limb-girdle muscular dystrophy 2C. *Muscle Nerve*. 2008; 37:308–316. [PubMed: 18041051]
39. Lynch GS. Role of contraction-induced injury in the mechanisms of muscle damage in muscular dystrophy. *Clin Exp Pharmacol Physiol*. 2004; 31:557–561. [PubMed: 15298551]
40. Zhu X, Hadhazy M, Wehling M, Tidball JG, McNally EM. Dominant negative myostatin produces hypertrophy without hyperplasia in muscle. *FEBS Lett*. 2000; 474:71–75. [PubMed: 10828454]
41. Welle S, Bhatt K, Pinkert CA, Tawil R, Thornton CA. Muscle growth after postdevelopmental myostatin gene knockout. *Am J Physiol Endocrinol Metab*. 2007; 292:E985–E991. [PubMed: 17148752]
42. Amthor H, Macharia R, Navarrete R, Schuelke M, Brown SC, Otto A, et al. Lack of myostatin results in excessive muscle growth but impaired force generation. *Proc Natl Acad Sci USA*. 2007; 104:1835–1840. [PubMed: 17267614]
43. McMahon CD, Popovic L, Oldham JM, Jeanplong F, Smith HK, Kambadur R, et al. Myostatin-deficient mice lose more skeletal muscle mass than wild-type controls during hindlimb suspension. *Am J Physiol Endocrinol Metab*. 2003; 285:E82–E87. [PubMed: 12618358]
44. Tsuchida K, Arai KY, Kuramoto Y, Yamakawa N, Hasegawa Y, Sugino H. Identification and characterization of a novel follistatin-like protein as a binding protein for the TGF-beta family. *J Biol Chem*. 2000; 275:40788–40796. [PubMed: 11010968]
45. Hill JJ, Qiu Y, Hewick RM, Wolfman NM. Regulation of myostatin in vivo by growth and differentiation factor-associated serum protein-1: a novel protein with protease inhibitor and follistatin domains. *Mol Endocrinol*. 2003; 17:1144–1154. [PubMed: 12595574]
46. Haidet AM, Rizo L, Handy C, Umaphathi P, Eagle A, Shilling C, et al. Long-term enhancement of skeletal muscle mass and strength by single gene administration of myostatin inhibitors. *Proc Natl Acad Sci USA*. 2008; 105:4318–4322. [PubMed: 18334646]
47. Ichikawa T, Zhang YQ, Kogure K, Hasegawa Y, Takagi H, Mori M, et al. Transforming growth factor beta and activin tonically inhibit DNA synthesis in the rat liver. *Hepatology*. 2001; 34:918–925. [PubMed: 11679962]
48. Goto Y, Nomura M, Tanaka K, Kondo A, Morinaga H, Okabe T, et al. Genetic interactions between activin type IIB receptor and Smad2 genes in asymmetrical patterning of the thoracic organs and the development of pancreas islets. *Dev Dyn*. 2007; 236:2865–2874. [PubMed: 17849440]

49. Xia Y, Sidis Y, Schneyer A. Overexpression of follistatin-like 3 in gonads causes defects in gonadal development and function in transgenic mice. *Mol Endocrinol.* 2004; 18:979–994. [PubMed: 14739256]
50. Mukherjee A, Sidis Y, Mahan A, Raheer MJ, Xia Y, Rosen ED, et al. FSTL3 deletion reveals roles for TGF-beta family ligands in glucose and fat homeostasis in adults. *Proc Natl Acad Sci USA.* 2007; 104:1348–1353. [PubMed: 17229845]
51. Artaza JN, Reisz-Porszasz S, Dow JS, Kloner RA, Tsao J, Bhasin S, et al. Alterations in myostatin expression are associated with changes in cardiac left ventricular mass but not ejection fraction in the mouse. *J Endocrinol.* 2007; 194:63–76. [PubMed: 17592022]
52. Cohn RD, Liang HY, Shetty R, Abraham T, Wagner KR. Myostatin does not regulate cardiac hypertrophy or fibrosis. *Neuromuscul Disord.* 2007; 17:290–296. [PubMed: 17336525]
53. Li ZF, Shelton GD, Engvall E. Elimination of myostatin does not combat muscular dystrophy in dy mice but increases postnatal lethality. *Am J Pathol.* 2005; 166:491–497. [PubMed: 15681832]
54. Parsons SA, Millay DP, Sargent MA, McNally EM, Molkentin JD. Age-dependent effect of myostatin blockade on disease severity in a murine model of limb-girdle muscular dystrophy. *Am J Pathol.* 2006; 168:1975–1985. [PubMed: 16723712]
55. Cooper BJ, Winand NJ, Stedman H, Valentine BA, Hoffman EP, Kunkel LM, et al. The homologue of the Duchenne locus is defective in X-linked muscular dystrophy of dogs. *Nature.* 1988; 334:154–156. [PubMed: 3290691]
56. Shimatsu Y, Yoshimura M, Yuasa K, Urasawa N, Tomohiro M, Nakura M, et al. Major clinical and histopathological characteristics of canine X-linked muscular dystrophy in Japan, CXMDJ. *Acta Myol.* 2005; 24:145–154. [PubMed: 16550932]
57. Harding TC, Koprivnikar KE, Tu GH, Zayek N, Lew S, Subramanian A, et al. Intravenous administration of an AAV-2 vector for the expression of factor IX in mice and a dog model of hemophilia B. *Gene Ther.* 2004; 11:204–213. [PubMed: 14712305]
58. Tsuchida K, Nakatani M, Hitachi K, Uezumi A, Sunada Y, Ageta H, et al. Activin signaling as an emerging target for therapeutic interventions. *Cell Commun Signal.* 2009; 7:15. [PubMed: 19538713]

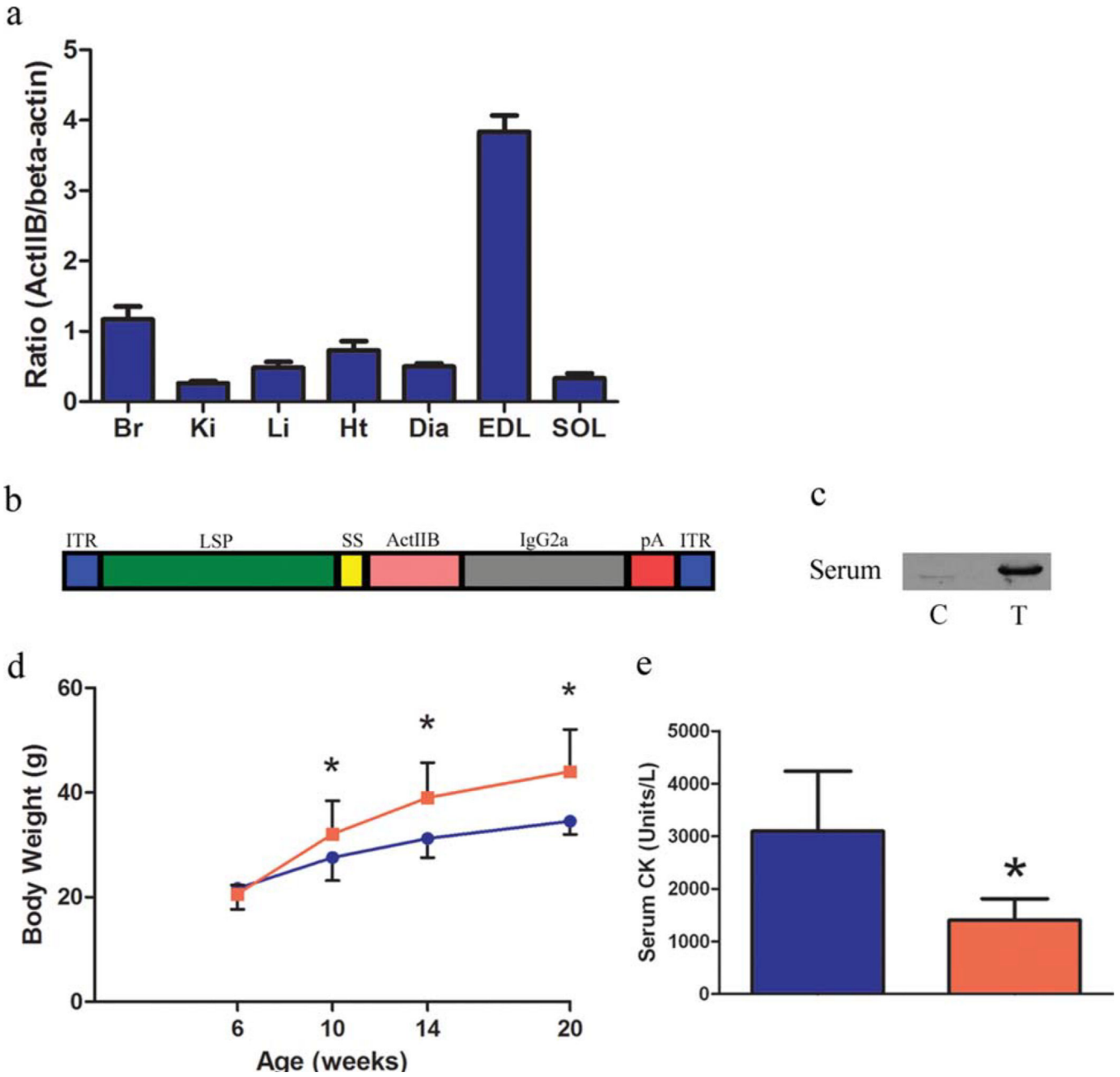


FIGURE 1. Expression of soluble activin IIB receptor in *mdx* mice. **(a)** Tissue distribution of the activin IIB receptor assessed by immunoblotting. **(b)** A schematic of the AAV construct used in this study. **(c)** Six-week-old *mdx* mice ($n = 5$ control, $n = 5$ treated) were injected intraperitoneally with $1E12$ genome copies of AAV 2/8 LSP.sActIIBr or saline. Immunoblotting of control (C) and treated (T) serum samples 1 month after injection demonstrates the presence of circulating sActIIBr. **(d)** Significantly increased body weight was noted in the *mdx*/sActIIBr group (shown in red) in comparison to control *mdx* mice (shown in blue) from 1 month post-injection until the conclusion of the study. **(e)** Activin receptor blockade significantly reduced serum CK from 3095 ± 1139 U/L in controls (blue

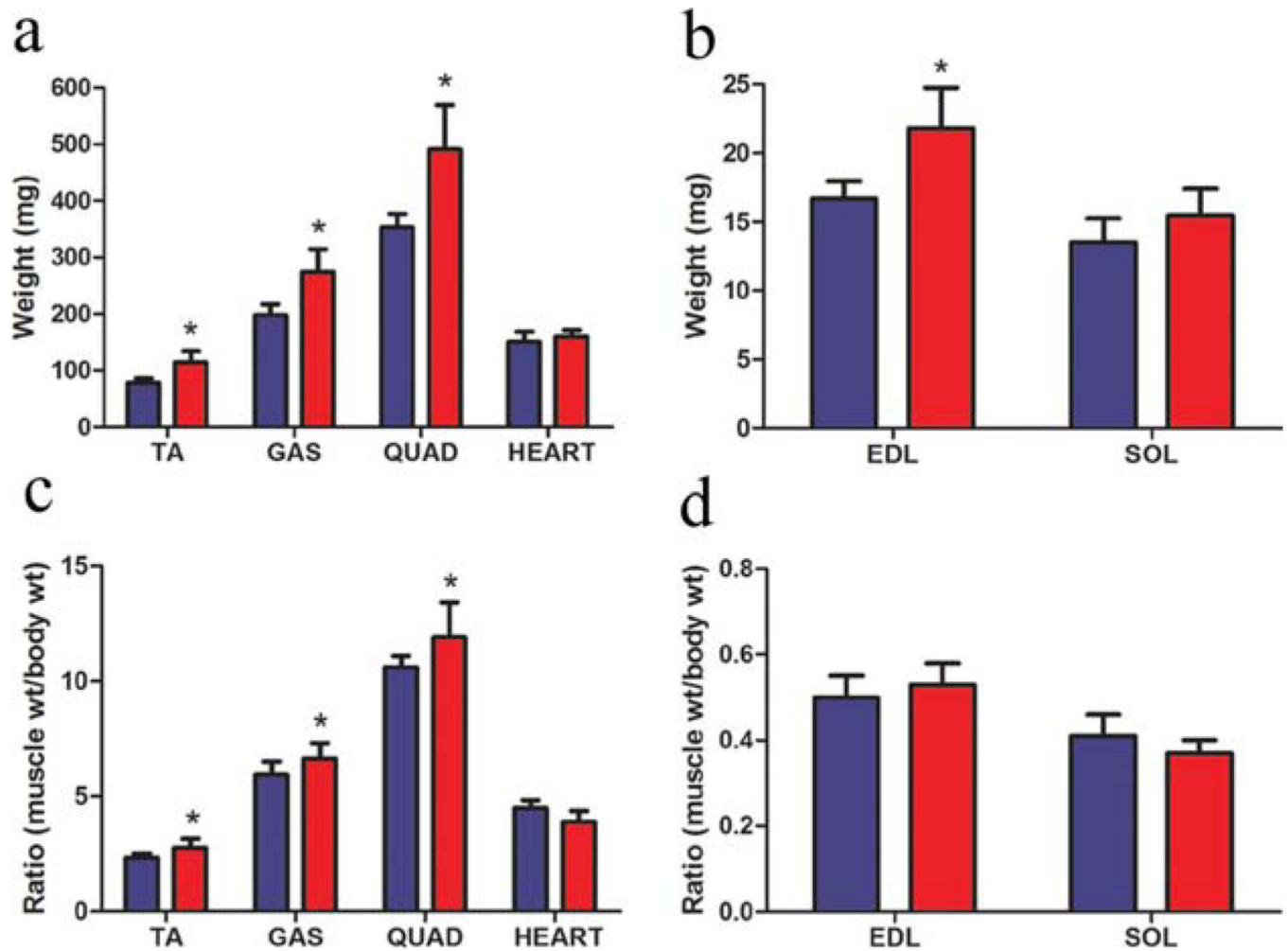
bar) to 1404 ± 409 U/L in treated mice (red bar). Br, brain; Ki, kidney; Li, liver; Ht, heart; Dia, diaphragm; EDL, extensor digitorum longus; SOL, soleus. $*P < 0.05$. [Color figure can be viewed in the online issue, which is available at wileyonlinelibrary.com.]

Author Manuscript

Author Manuscript

Author Manuscript

Author Manuscript

**FIGURE 2.**

Effect of soluble ActIIbR expression on muscle weight in *mdx* mice. (a) Treatment with sActIIbR increased the muscle mass of the tibialis anterior (TA) by 46%, the gastrocnemius (GAS) by 39%, and the quadriceps (QUAD) by 39%. No difference in heart weight was observed in the *mdx/sActIIbR* group. (b) The EDL demonstrated a 31% gain of muscle mass, whereas the soleus (SOL) wet weight did not change. (c, d) The ratio of muscle weight to body weight was increased in the TA, GAS, and QUAD muscles, whereas the ratio was unchanged in the heart, EDL, and soleus. Blue bars represent data from control *mdx* mice ($n = 5$); red bars represent data from *mdx/sActIIbR* mice ($n = 5$). * $P < 0.05$. TA, tibialis anterior; GAS, gastrocnemius; QUAD, quadriceps; SOL, soleus. [Color figure can be viewed in the online issue, which is available at wileyonlinelibrary.com.]

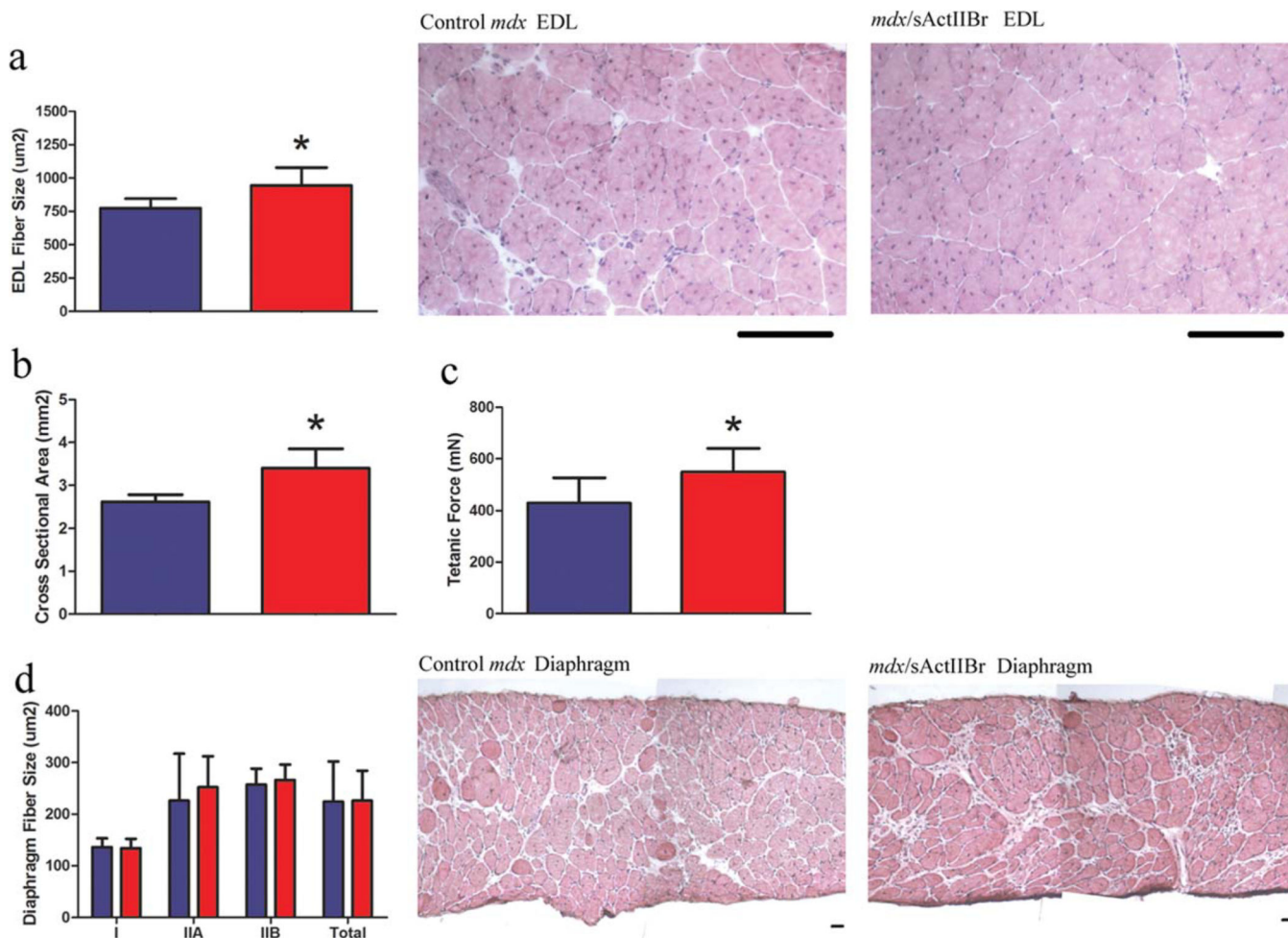


FIGURE 3.

Morphometric and functional properties of the EDL and diaphragm. **(a)** The mean fiber size of the EDL was larger in the *mdx/sActIIBr* group. Representative hematoxylin and eosin–stained muscle sections are shown. Scale bar: 100 µm. **(b)** The cross-sectional area of the EDL was increased from 2.6 ± 0.2 to 3.4 ± 0.5 µm² in treated mice. **(c)** An increase in tetanic force production (430 ± 96 vs. 549 ± 91 mN) was observed in the treated EDL. **(d)** In the diaphragm, the mean fiber sizes of type I, type IIA, type IIB, and total fibers were not altered by overexpression of soluble activin receptor. Representative hematoxylin and eosin–stained muscle sections are shown. Scale bar: 50 µm. Blue bars represent data from control *mdx* mice ($n = 5$); red bars represent data from *mdx/sActIIBr* mice ($n = 5$). * $P < 0.05$. [Color figure can be viewed in the online issue, which is available at wileyonlinelibrary.com.]